Theoretical Studies of Elimination Reactions. 1. Reactions of F^- and PH_2^- with CH_3CH_2Cl. Competition between S_N2 and E2 Mechanisms for First- and Second-Row Nucleophiles

Scott Gronert

Contribution from the Department of Chemistry and Biochemistry, San Francisco State University, San Francisco, California 94132. *Received January 14, 1991*

Abstract: In this study the gas-phase reactions of F^- and PH_2^- (proton affinities 371.5 and 370.9 kcal mol, respectively) with CH_3CH_2Cl were characterized with ab initio methods. For each nucleophile, S_N2, E2(anti), and E2(syn) reaction paths were investigated and transition-state structures were located. At the MP4SDQ/6-31(+)G**//HF/6-31(+)G* level of theory, activation barriers were calculated. Analytical frequencies were computed for each transition state and minimum, and all energies are corrected for zero-point vibrations (scaled by 0.9). With F^- as the nucleophile, negative activation barriers (-6.7 and -5.7 kcal/mol, respectively) were found for the S_N2 and E2(anti) reactions, indicating that substitution and elimination should be competitive. A positive activation barrier of +7.0 kcal/mol was found for the E2(syn) reaction, indicating a strong preference for an antiperiplanar transition state. With PH_2^-, the S_N2 reaction has a small activation barrier (+5.8 kcal/mol), but the E2(anti) and E2(syn) have very large activation barriers (+17.4 and +25.8 kcal/mol). Although F^- and PH_2^- have nearly the same thermodynamic basicities, their abilities to induce elimination reactions are very different. The theoretical results are consistent with recent gas-phase studies which indicate that first-row nucleophiles are well-suited for both S_N2 and E2 reactions whereas second-row nucleophiles are more limited to S_N2 reactions. Atomic electron populations and critical point densities were computed with Bader's method and are used to develop a model that explains the nucleophilic preferences in terms of bond polarities.

Introduction

The S_N2 and E2 reactions are fundamental examples in mechanistic organic chemistry, yet questions remain about the structures and energetics of their transition states. In particular, what are the factors that affect the competition between the two reaction pathways. Solution-phase studies have led to a tremendous literature for both reactions,[1-6] yet solvent and ion pairing effects in these studies can mask important mechanistic details. Realizing that chemists generally view mechanism in terms of bonding changes in a solvent-free environment (consider the "standard" S_N2 and E2 mechanisms in Figure 1), it is clear that theoretical and gas-phase studies offer two of the most useful and important approaches to probing mechanism.[7-14]

Literally dozens of theoretical papers have centered on the S_N2 reaction, and a wide variety of nucleophile/leaving group partners have been investigated. In fact, the S_N2 is probably the most thoroughly studied and analyzed reaction in theoretical organic chemistry.[15-18] In contrast, relatively little theoretical work has been reported on the E2 reaction.[16,19-21] The major reason for

(1) For E2 reactions, see: (a) Bartsch, R. A.; Zavada, J. *Chem. Rev.* **1980**, *80*, 454. (b) Bartsch, R. A. *Acc. Chem. Res.* **1975**, *8*, 128. (c) Ingold, C. K. *Structure and Mechanism in Organic Chemistry*, 2nd ed.; Cornell University Press: Ithaca, NY, 1969. (d) Saunders, W. H., Jr.; Cockerill, A. F. *Mechanism of Elimination Reactions*; Wiley-Interscience: New York, 1973; Chapter 1. (e) Saunders, W. H., Jr. *Acc. Chem. Res.* **1976**, *8*, 19. (f) Saunders, W. H., Jr. *The Chemistry of Alkenes*; Patai, S., Ed.; Wiley-Interscience: New York, 1964. (g) Baciocchi, E. *Acc. Chem. Res.* **1979**, *12*, 430. (h) Cordes, E. H.; Jencks, W. P. *J. Am. Chem. Soc.* **1963**, *85*, 2843. (i) Banthorpe, D. V. *Reaction Mechanism in Organic Chemistry*; Hughes, E. D., Ed.; Elsevier: London, 1963; Vol. 2 (Elimination Reactions).

(2) (a) Bunnett, J. F. *Angew. Chem., Int. Ed. Engl.* **1962**, *1*, 225. (b) Bartsch, R. A.; Bunnett, J. F. *J. Am. Chem. Soc.* **1968**, *90*, 408.

(3) (a) Beltrame, P.; Biale, G.; Lloyd, D. J.; Parker, A. J.; Ruane, M.; Winstein, S. *J. Am. Chem. Soc.* **1972**, *94*, 2240. (b) Parker, A. J.; Ruane, M.; Palmer, D. A.; Winstein, S. *J. Am. Chem. Soc.* **1972**, *94*, 2228.

(4) Cram, D. J.; Greene, F. D.; DePuy, C. H. *J. Am. Chem. Soc.* **1956**, *78*, 790.

(5) (a) Sicher, J. *Angew. Chem., Int. Ed. Engl.* **1972**, *11*, 200. (b) Wolfe, S. *Acc. Chem. Res.* **1972**, *5*, 102. (c) DePuy, C. H.; Thurn, R. D.; Morris, G. F. *J. Am. Chem. Soc.* **1962**, *84*, 1314.

(6) For S_N2 reactions, see: (a) Bunton, C. A. *Nucleophilic Substitution at a Saturated Carbon Atom*; Elsevier: Amsterdam, 1963. (b) Ingold, C. K. *Structure and Mechanism in Organic Chemistry*; Cornell University Press: Ithaca, NY, 1969. (c) Harris, J. M. *Prog. Phys. Org. Chem.* **1974**, *11*, 89. (d) Bentley, T. W.; Schleyer, P. v. R. *Adv. Phys. Org. Chem.* **1977**, *14*, 1. (e) Parker, A. J. *Chem. Rev.* **1969**, *69*, 1. (f) Pearson, R. G.; Sobel, H.; Songstad, J. *J. Am. Chem. Soc.* **1968**, *90*, 319. (g) Lowry, T. H.; Richardson, K. S. *Mechanism and Theory in Organic Chemistry*; Harper & Row: New York, 1987.

(7) (a) DePuy, C. H.; Gronert, S.; Mullin, A.; Bierbaum, V. M. *J. Am. Chem. Soc.* **1990**, *112*, 8650. (b) Gronert, S.; DePuy, C. H.; Bierbaum, V. M. *J. Am. Chem. Soc.* **1991**, *113*, 4009.

(8) Jones, M. E.; Ellison, G. B. *J. Am. Chem. Soc.* **1989**, *111*, 1645.

(9) Lieder, C. A.; Brauman, J. I. *Int. J. Mass Spectrom. Ion Phys.* **1975**, *16*, 307.

(10) (a) Riveros, J. M.; Jose, S. M.; Takashima, I. *Adv. Phys. Org. Chem.* **1985**, *21*, 197 and references therein. (b) Lum, R. C.; Grabowski, J. J. *J. Am. Chem. Soc.* **1988**, *110*, 8568. (c) DePuy, C. H.; Bierbaum, V. M. *J. Am. Chem. Soc.* **1981**, *103*, 5034. (d) DePuy, C. H.; Beedle, E. C.; Bierbaum, V. M. *J. Am. Chem. Soc.* **1982**, *104*, 6483. (e) de Koning, L. J.; Nibbering, N. M. M. *J. Am. Chem. Soc.* **1987**, *109*, 1715. (f) Faigle, J. F. G.; Isolani, P. C.; Riveros, J. M. *J. Am. Chem. Soc.* **1976**, *98*, 2049. (g) King, G. K.; Maricq, M. M.; Bierbaum, V. M.; DePuy, C. H. *J. Am. Chem. Soc.* **1981**, *103*, 7133. (h) Noest, A. J.; Nibbering, N. M. M. *Adv. Mass Spectrom.* **1980**, *8*, 227. (i) Bartmess, J. E.; Hays, R. L.; Khatri, H. N.; Misra, R. N.; Wilson, S. R. *J. Am. Chem. Soc.* **1981**, *103*, 4746.

(11) (a) Bohme, D. K.; MacKay, G. I. *J. Am. Chem. Soc.* **1981**, *103*, 978. (b) Bohme, D. K.; Raskit, A. B. *Can. J. Chem.* **1985**, *63*, 3007.

(12) (a) Olmstead, W. N.; Brauman, J. I. *J. Am. Chem. Soc.* **1977**, *99*, 4219. (b) Pellerite, M. J.; Brauman, J. I. *J. Am. Chem. Soc.* **1983**, *105*, 2672.

(13) Barlow, S. E.; Van Doren, J. M.; Bierbaum, V. M. *J. Am. Chem. Soc.* **1988**, *110*, 7240.

(14) (a) Sullivan, S. A.; Beauchamp, J. L. *J. Am. Chem. Soc.* **1977**, *99*, 5017. (b) Sullivan, S. A.; Beauchamp, J. L. *J. Am. Chem. Soc.* **1976**, *98*, 1160. (c) Ridge, D. P.; Beauchamp, J. L. *J. Am. Chem. Soc.* **1974**, *96*, 637.

(15) (a) Tucker, S. C.; Truhlar, D. G. *J. Am. Chem. Soc.* **1990**, *112*, 3338. (b) Tucker, S. C.; Truhlar, D. G. *J. Phys. Chem.* **1989**, *93*, 8138.

(16) (a) Minato, T.; Yamabe, S. *J. Am. Chem. Soc.* **1988**, *110*, 4586. (b) Minato, T.; Yamabe, S. *J. Am. Chem. Soc.* **1985**, *107*, 4621.

(17) For example, see: (a) Vande Linde, S. R.; Hase, W. L. *J. Am. Chem. Soc.* **1989**, *111*, 2349. (b) Sand, P.; Bergman, J.; Lindholm, E. *J. Phys. Chem.* **1988**, *92*, 2039. (c) Urban, M.; Diercksen, G. H. F.; Cernusak, I.; Havlas, Z. *Chem. Phys. Lett.* **1989**, *159*, 153. (d) Merkel, A.; Havlas, Z.; Zahradnik, R. *J. Am. Chem. Soc.* **1988**, *110*, 8355. (e) Vetter, R.; Zulicke, L. *J. Mol. Struct. (Theochem)* **1988**, *170*, 85. (f) Carrion, F.; Dewar, M. J. S. *J. Am. Chem. Soc.* **1984**, *106*, 3531. (g) Chandrasekhar, J.; Smith, S. F.; Jorgensen, W. L. *J. Am. Chem. Soc.* **1985**, *107*, 154. (h) Evanseck, J. D.; Blake, J. F.; Jorgensen, W. L. *J. Am. Chem. Soc.* **1987**, *109*, 2349. (i) Mitchell, D. J.; Schlegel, H. B.; Shaik, S. S.; Wolfe, S. *Can. J. Chem.* **1985**, *63*, 1642. (j) Shaik, S. S.; Pross, A. *J. Am. Chem. Soc.* **1982**, *104*, 2708.

(18) Shi, Z.; Boyd, R. J. *J. Am. Chem. Soc.* **1990**, *112*, 6789 and references therein.

(19) (a) Dewar, M. J.; Yuan, Y.-C. *J. Am. Chem. Soc.* **1990**, *112*, 2088. (b) Dewar, M. J.; Yuan, Y.-C. *J. Am. Chem. Soc.* **1990**, *112*, 2095.

(20) Bach, R. D.; Badger, R. C.; Lang, T. J. *J. Am. Chem. Soc.* **1979**, *101*, 2845.

0002-7863/91/1513-6041$02.50/0

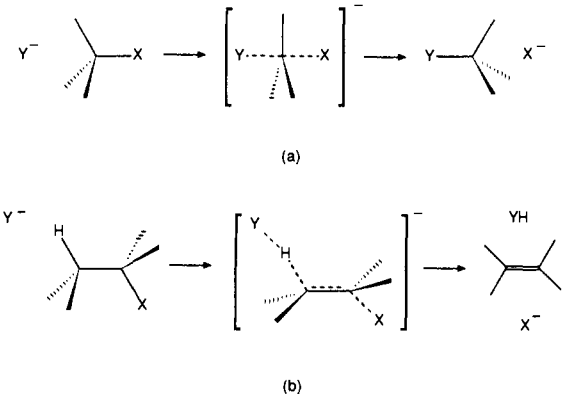

Figure 1. Typical Representations of (a) S_N2 and (b) E2(anti) mechanisms.

this imbalance is the complex nature of the E2 transition state. In the S_N2 reaction a bond is broken and formed in a concerted fashion, whereas in the E2 process, four simultaneous bonding changes occur (two forming and two breaking). Since the bonding changes are not necessarily synchronous, a variety of transition-state structures are possible. On the basis of the work of Bunnett[2] and Cram,[4] it is known that the transition state for a bimolecular elimination may vary from $E1_{cb}$-like to E1-like with the prototypic E2-type transition state at the center of this spectrum. Because the reaction path is much more complex, locating and optimizing the transition-state structure of an E2 elimination involves a far more challenging procedure than is required for an S_N2 reaction.

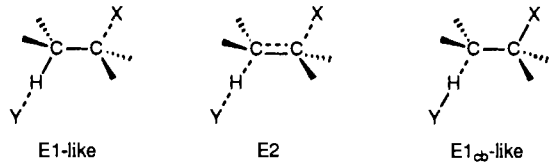

An additional complication is that E2 reactions can involve either syn or anti periplanar conformations in the transition state.[5] A few theoretical studies of E2 reactions are available, but only a limited number of nucleophiles have been considered and the calculations have been at low levels generally. In early work, Bach et al. considered the E2 reaction of H^- with CH_3CH_2F via anti and syn configured transition states.[20] Minato and Yamabe[16] have reported transition-state structures for the reactions of F^- and Cl^- with CH_3CH_2F and CH_3CH_2Cl, but these calculations employed relatively small basis sets (3-21G). Very recently, Dewar and co-workers[19] used the AM1 method to investigate a variety of E2 eliminations initiated with methoxide and ammonia as nucleophiles; however, the ability of semiempirical techniques to adequately characterize these complicated systems is unknown.

In a recent, comprehensive study of gas-phase reactions of nucleophiles with alkyl halides, DePuy et al.[7] have reported an interesting reactivity pattern in E2 and S_N2 reactions. Their work indicates that the competition between S_N2 and E2 pathways is dependent not only on the basicity of the nucleophile but also on the nature of the nucleophilic atom. In the reactions of fluorinated alkoxides with alkyl chlorides and bromides, reaction rates generally increase with greater substitution at the α-carbon, indicating that E2 as well as S_N2 pathways are active. The presence of large primary deuterium isotope effects ($\sim$4) in the reactions of labeled secondary and tertiary alkyl halides with the fluorinated alkoxides is clear evidence that the E2 pathway is important and probably dominates with highly substituted alkyl halides. In contrast, sulfur-based nucleophiles (HS^- and H_2NS^-) react readily with methyl halides, but only sluggishly or not at all with secondary and tertiary chlorides and bromides even though these sulfur nucleophiles have nearly the same gas-phase basicities as the fluorinated alkoxides. The absence of primary deuterium isotope effects in the reactions of sulfur nucleophiles with labeled substrates provides further evidence that E2 pathways are not important with these nucleophiles. With methyl chloride and bromide the sulfur and oxygen nucleophiles give more similar reaction rates (oxygen nucleophiles react about twice as fast); consequently, the S_N2 path is not as sensitive to the nature of the nucleophilic atom.

In the present study, ab initio methods are used to probe the gas-phase mechanisms of E2 eliminations and S_N2 displacements. In particular, the role that the nucleophile plays in determining the reaction path (E2 or S_N2) is investigated. The study involves comparing the ability of representative first- and second-row nucleophiles to undergo S_N2 and E2 reactions and analyzing the roots of their mechanistic preferences. For a fair comparison, the first- and second-row nucleophiles must have similar gas-phase basicities or, equivalently, similar E2 reaction exothermicities. Otherwise, kinetic and thermodynamic effects cannot be separated. For example, Minato and Yamabe[16] considered the reactions of F^- and Cl^- with CH_3CH_2Cl, but because the E2 reaction with F^- is 40 kcal/mol more exothermic than the corresponding reaction with Cl^-, no direct comparisons can be made. In addition, the nucleophiles must have simple structures so that high-level theoretical calculations are practical. Given these criteria, F^- and PH_2^- (PA = 371.5 and 370.9 kcal/mol, respectively)[22] are the most reasonable choices. Ethyl chloride was chosen as the substrate because it is the simplest, realistic alkyl halide capable of both S_N2 and E2 reactions. To fully characterize these systems and compare E2 and S_N2 barriers, transition-state structures were located for both the anti and syn eliminations as well as the S_N2 displacements of F^- and PH_2^- with CH_3CH_2Cl.

An attractive aspect of theoretical chemistry is the ability to characterize the electron distributions of molecules. Unfortunately, abstracting atomic populations from an electronic wave function is not straightforward. Ideally, electron density could be assigned uniquely and unambiguously to each atom; however, because covalent systems naturally involve shared electron density, an arbitrary partitioning scheme must be applied to define atomic populations. Two fundamentally different approaches have been applied in the past. One approach relies on a partitioning based on orbital occupancy (Mulliken[23] and more recently "natural populations"[24]) and the other on a partitioning in space (Bader[25] and Streitwieser integrated populations[26]). Methods based on orbital occupancy are easily applied, yet are known to be basis set dependent (particularly Mulliken populations)[27] and have been criticized often in the literature. The better approach is to define atomic volumes within the molecule and determine populations by integrating the electron density within these volumes. This approach limits basis set dependencies and is based on the intuitive assumption that electron density near an atom is associated with that atom.

Over the past two decades, Bader and co-workers have developed a procedure for uniquely assigning atomic volumes and integrating them to yield atomic populations.[25] This method is related to Streitwieser's integrated populations,[26] but it uses a more rigorously defined volume and a full 3-dimensional integration. For this study, the Bader approach has been applied to determine electron populations. Although populations of this type are rigorously defined, one must be careful in their interpretation. The

(21) Pross, A.; Shaik, S. S. *J. Am. Chem. Soc.* **1982**, *104*, 187.

(22) Lias, S. G.; Bartmess, J. E.; Liebman, J. F.; Holmes, J. L.; Levin, R. D.; Mallard, W. G. *J. Phys. Chem. Ref. Data* **1988**, *17*, Suppl. No. 1.

(23) Mulliken, R. S. *J. Chem. Phys.* **1955**, *23*, 1833, 1841, 2338, 2343.

(24) (a) Reed, A. E.; Weinstock, R. B.; Weinhold, F. *J. Chem. Phys.* **1985**, *83*, 735. (b) Reed, A. E.; Weinhold, F. *J. Am. Chem. Soc.* **1986**, *108*, 3586. (c) Reed, A. E.; Weinhold, F. *J. Am. Chem. Soc.* **1985**, *107*, 1919.

(25) For recent descriptions, see: (a) Bader, R. F. W. *Acc. Chem. Res.* **1985**, *18*, 9. (b) Bader, R. F. W.; Nguyen-Dang, T. T. *Adv. Quantum Chem.* **1981**, *14*, 63. (c) Wiberg, K. B.; Bader, R. F. W.; Lau, C. D. H. *J. Am. Chem. Soc.* **1987**, *109*, 985.

(26) (a) Collins, J. B.; Streitwieser, A., Jr. *J. Comput. Chem.* **1980**, *1*, 81. (b) McDowell, R. S.; Grier, D. L.; Streitwieser, A., Jr. *J. Comput. Chem.* **1985**, *9*, 165.

(27) For example, see: (a) Bachrach, S. M.; Streitwieser, A., Jr. *J. Am. Chem. Soc.* **1984**, *106*, 2283. (b) Bachrach, S. M.; Streitwieser, A., Jr. *J. Comput. Chem.* **1989**, *10*, 514. (c) Gronert, S.; Glaser, R.; Streitwieser, A., Jr. *J. Am. Chem. Soc.* **1989**, *111*, 3111.

Table I. Structures and Energies of Nucleophiles and Conjugate Acids

	geometry		HF	MP2	MP3	MP4
F^-		energies[a]	−99.418 586	−99.623 847	−99.613 630	−99.623 35
		proton affinity[b]	374.3	365.5	371.4	368.1
PH_2^-	P–H, 1.425 Å H–P–H, 93.46°	energies[a]	−341.857 647	−341.980 521	−341.998 968	−342.002 052
		proton affinity[b]	367.7	369.1	370.9	371.4
HF	H–F, 0.911 Å	energies[a]	−100.024 208	−100.215 533	−100.214 721	−100.219 187
PH_3	P–H, 1.403 Å H–P–H, 95.40°	energies[a]	−342.455 031	−342.580 199	−342.601 574	−342.605 347

[a] Anions are optimized at the 6-31(+)G* level and neutrals at the 6-31G* level. Energy calculations involve a 6-31(+)G** single-point calculation on the above optimized structures. Energies in hartrees. [b] Proton affinities in kcal/mol corrected with zero-point energies scaled by 0.9.

populations represent the density within a defined volume, and atomic charges determined in this way should not be used to develop an "ionic" representation of the molecule. Partial positive and negative charges indicate that the shared density is polarized and therefore closer to one of the bonding atoms. This highlights the importance of an ionic resonance form in describing the bond, but it does not imply that the bond is purely ionic (lacking shared density). Population analysis, when applied to ostensibly covalent molecules, gives a measure of the bond polarization and, therefore, is an exceptionally useful tool for characterizing the shifts in electron density which accompany chemical transformations.

Calculations

All calculations were carried out on a Multi-Flow-Trace14 computer with use of the GAUSSIAN 88 quantum mechanical package developed by Pople and co-workers.[28] All structures were fully optimized without symmetry constraints with use of a variety of basis sets derived from the standard 6-31G* basis.[29] For anionic systems, diffuse sp orbitals were placed on all centers expected to bear a significant negative charge. For systems **1**, **2**, **3**, and **4**, diffuse functions were placed on fluorine and chlorine, and for systems **5**, **6**, **7**, and **8**, they were placed on phosphorus and chlorine.[30,31] These basis sets will be designated as 6-31(+)G* in the text. Neutral systems were optimized with the standard 6-31G* basis set. The curvature of the potential energy surface at all minima and transition states was confirmed with analytical second derivatives and frequencies are reported in the supplementary material. For energy comparisons, single-point calculations were done on the optimized geometries with use of a basis set that included polarization (p) functions on the hydrogens, 6-31(+)G**.[32] To correct for correlation effects, frozen-core Moeller–Plesset perturbation theory was applied up to the fourth level allowing single, double, and quadruple excitations (MP4SDQ).[33] Energies also are corrected for zero-point energy differences (scaled by 0.9).[34]

Integrated electron populations and critical point densities were calculated with Bader's PROAIM package modified to run on a Sun 4/110 workstation. The details of these calculations have been described elsewhere.[25]

Results and Discussion

Proton Affinities of F^- and PH_2^-. To check the accuracy of the basis sets and level of theory, the gas-phase proton affinities (PA) of F^- and PH_2^- were calculated and compared to experimental values. In this way, it is possible to assess the ability of the ab initio calculation to represent the nucleophile and its bonding interactions. The gas-phase proton affinity of F^- is very well known and has a value of 371.5 ± 0.2 kcal/mol. A less precise value has been reported for PH_2^- (PA = 370.9 ± 2.0 kcal/mol) in the gas phase.[22]

The optimized structures of PH_3, HF, and PH_2^- are given in Table I. At the HF/6-31(+)G** level, the calculated proton affinity of F^- is 374.3 kcal/mol, approximately 3 kcal/mol above the experimental value. The incorporation of Moeller–Plesset (MP) corrections leads to a slow convergence series (see Table I) which appears to be approaching a value of about 369 or 370 kcal/mol; at the highest level (MP4SDQ), the proton affinity is 368.1 kcal/mol. For PH_2^-, the PA at the Hartree–Fock level is 367.7 kcal/mol or about 3 kcal/mol below the experimental value. Addition of MP corrections leads to a smooth progression toward the experimental value with all the MP results falling within the experimental uncertainties.

The test calculations clearly indicate that the present level of theory is adequate for qualitative/quantitative analyses. In addition, Shi and Boyd[18] have found that although Moeller–Plesset corrections are required for accurate energy calculations on S_N2 transition states, Hartree–Fock optimized geometries are adequate. On the basis of the test calculations, one would expect that the energies in this study would be reliable to within a few kcal/mol. This accuracy is sufficient to determine the energetic viability of various reaction pathways, but quantitative estimates of reaction rates would require higher levels of theory.

Ion–Dipole Complexes. First, consider the reaction of fluoride with ethyl chloride. Minato and Yamabe[16] examined this reaction at the 3-21G level and their results are generally consistent with the present 6-31(+)G* results. In the gas phase, the first minimum along the reaction coordinate is usually a weakly bound, ion–dipole complex. The initial reaction product of F^- and CH_3CH_2Cl is an ion–dipole complex, **1**, with the F^- situated at the backside of the C–Cl bond and weakly hydrogen bonded to a β hydrogen (anti); the H_β–F distance is 2.2 Å (Figure 2). In the ion–dipole complex, the geometry of the CH_3CH_2Cl is only slightly perturbed, and the interaction of the F^- with the backside of the C–Cl bond leads to a small bond elongation (C–Cl = 1.87 Å in **1**, 1.80 Å in CH_3CH_2Cl). At the MP4SDQ/6-31(+)G**//HF/6-31(+)G* level this complex lies 15.1 kcal/mol below the energy of the separated reactants. This value is typical of gas-phase ion–dipole complexes[35] and similar to the experimental value (12.2 kcal/mol) that Larson and McMahon found for the related system, chloride–methyl chloride.[36] Minato and Yamabe[16] found a second minimum where the F^- is hydrogen bonded to a β hydrogen (C–H_β–F angle = ~180°) but does not interact with the C–Cl bond; however, at the 6-31(+)G* level structures of this type collapse to **1**. A similar structure, **5**, is observed when PH_2^- is allowed to complex with CH_3CH_2Cl. Again, the nucleophile interacts with both the C–Cl bond and a β hydrogen, but the complexation energy, 7.7 kcal/mol, is significantly lower. The low complexation energy is probably a reflection of the delocalized

(28) GAUSSIAN 88: Frisch, M. J.; Head-Gordon, M.; Schlegel, H. B.; Raghavachari, K.; Binkley, J. S.; Gonzalez, C.; DeFrees, D. J.; Fox, D. J.; Whiteside, R. A.; Seeger, R.; Melius, C. F.; Baker, J.; Martin, R. L.; Kahn, L. R.; Stewart, J. J. P.; Fleuder, E. M.; Topiol, S.; Pople, J. A. Gaussian, Inc., Pittsburgh, PA.

(29) (a) Hariharan, P. C.; Pople, J. A. *Theor. Chim. Acta* **1973**, *28*, 213. (b) Dill, J. D.; Pople, J. A. *J. Chem. Phys.* **1975**, *62*, 2921. (c) Francl, M. M.; Pietro, W. J.; Hehre, W. J.; Gordon, M. S.; DeFrees, D. J.; Pople, J. A. *J. Chem. Phys.* **1982**, *77*, 3654.

(30) (a) Clark, T.; Chandrasekhar, J.; Spitznagel, G. W.; Schleyer, P. v. R. *J. Comput. Chem.* **1983**, *4*, 294. (b) Spitznagel, G. W.; Clark, T.; Chandrasekhar, J.; Schleyer, P. v. R. *J. Comput. Chem.* **1982**, *3*, 363.

(31) Diffuse functions were added to the β-carbon in a test calculation of E2 transition-state **4**. Although this transition state has significant $E1_{cb}$ character, the diffuse functions had negligible effects on the structure and relative energy. In addition, diffuse functions on hydrogen had little affect on the proton affinity of PH_2^-.

(32) For a full discussion of these basis sets, see: Hehre, W. J.; Radom, L.; Schleyer, P. v. R.; Pople, J. A. *Ab Initio Molecular Orbital Theory*; Wiley: New York, 1986; also references therein.

(33) DeFrees, D. J.; Levi, B. A.; Pollack, S. K.; Hehre, W. J.; Binkley, J. S.; Pople, J. A. *J. Am. Chem. Soc.* **1979**, *101*, 4085.

(34) Pople, J. A.; Schlegel, H. B.; Krishnan, R.; DeFrees, D. J.; Binkley, J. S.; Frisch, M. J.; Whiteside, R. A.; Hout, R. F.; Hehre, W. J. *Int. J. Quantum Chem. Symp.* **1981**, *15*, 269.

(35) Su, T.; Bowers, M. T. In *Gas Phase Ion Chemistry*; Bowers, M. T., Ed.; Academic Press: New York, 1979; Vol. I.

(36) Larson, J. W.; McMahon, T. B. *J. Am. Chem. Soc.* **1985**, *107*, 766.

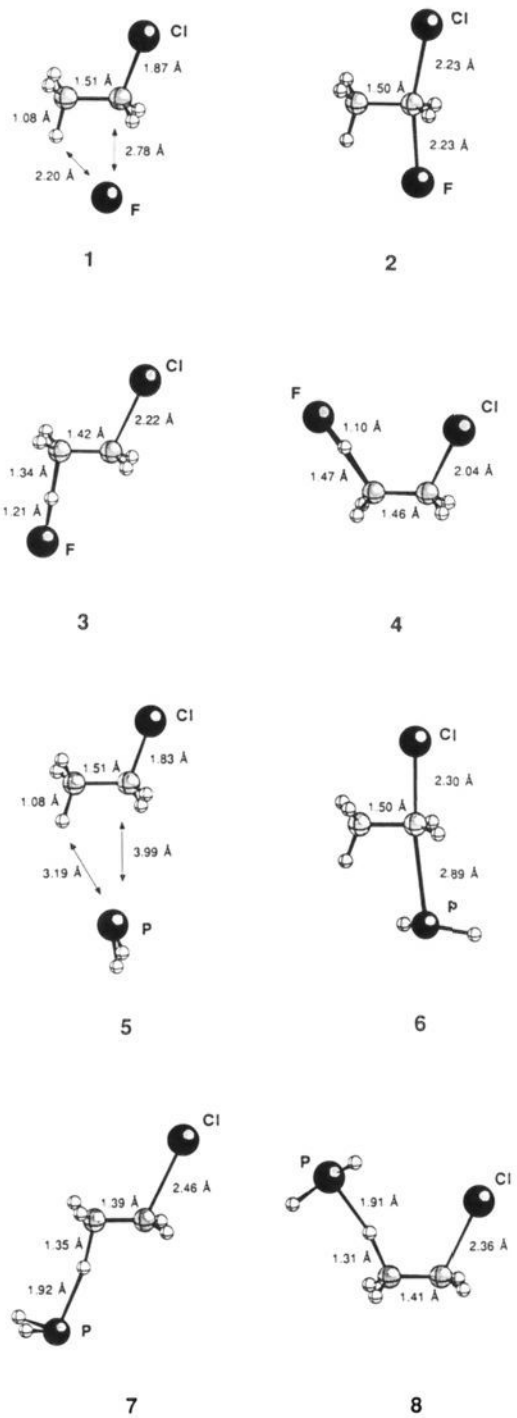

Figure 2. Structures of minima and transition states.

nature of the phosphide anion.[37] From complexes **1** and **5**, these systems are poised to undergo either S_N2 displacements or anti E2 eliminations.

S_N2 Transition States. The transition state for the S_N2 reaction of F^- with CH_3CH_2Cl (**2**) was located by using analytical second derivatives and contains a single negative frequency (−415 cm^{-1}). The structure (Figure 2) is characterized by a long C–F distance (2.23 Å) and a relatively small elongation of the C–Cl bond (2.23 Å compared to 1.80 Å in CH_3CH_2Cl). The geometry is consistent with the Hammond postulate[38] of early transition states for exothermic reactions ($\Delta H°$ = −29.0 kcal/mol).[39] The early transition state also is evident in the hybridization of the α-carbon which still is pyramidalized away from the Cl. The bond lengths in **2** can be compared to those found in the transition state of the analogous reaction of F^- with CH_3Cl. Shi and Boyd[18] recently have reported C–Cl and C–F bond lengths of 2.13 and 2.13 Å, respectively, from a 6-31++G** optimization of that S_N2 transition state. The longer C–F and C–Cl bonds found in **2** are evidence of minor steric crowding by the methyl group.

Next, it is interesting to consider how the structural changes leading to the transition state are reflected in changes in the electron density distribution. Using Bader's method of molecular partitioning (Table II), we find that the leaving Cl in **2** has excess electron density (17.72 e^-) and, as a result, a negative charge (−0.72) in the transition state. By comparison to the value obtained in CH_3CH_2Cl (17.34 e^-), it is clear that significant charge transfer to the Cl already has occurred at the transition state. This is balanced by only a small charge transfer from the F^- (10 e^- in F^- to 9.94 e^- in **2**). The net result is a relatively large positive charge, +0.66, on the CH_3CH_2 fragment. This is consistent with earlier work by Bader[40] which showed that S_N2 transition states are characterized by negative charges on the entering and leaving groups and a large positive charge on the intervening carbon. The Mulliken populations for **2** are given in Table II and generally are similar to the values derived from Bader-type analyses. Be-

Table II. Integrated Atomic Populations[a]

structure	element	n^b	net charge	Mulliken charges
2	F	9.94	−0.94	−0.88
	Cl	17.72	−0.72	−0.65
3	F	9.88	−0.88	−0.79
	Cl	17.71	−0.71	−0.63
	H_β	0.42	+0.58	+0.46
	C_β	5.99	+0.01	−0.51
4	F	9.88	−0.88	−0.80
	Cl	17.58	−0.58	−0.46
	H_β	0.33	+0.67	+0.63
	C_β	6.16	−0.16	−0.70
6	PH_2[c]	17.75	−0.75	−0.81
	H(P)[e]	1.60	−0.60	−0.11
	Cl	17.73	−0.73	−0.68
7	PH_2	17.60	−0.60	−0.56
	H(P)[e]	1.65	−0.65	−0.07
	Cl	17.81	−0.81	−0.78
	H_β	0.76	+0.24	+0.15
	C_β	5.93	+0.07	−0.54
8	*PH_2*	*17.46*	*−0.46*	*−0.55*
	H(P)[e]	1.58	−0.58	−0.08
	Cl	17.74	−0.74	−0.67
	H_β	0.74	+0.26	+0.20
	C_β	5.96	+0.04	−0.59
CH_3CH_2Cl[d]	Cl	17.34	−0.34	−0.13
	C_β	5.76	+0.24	−0.34
	H_β	1.06	−0.06	+0.17
CH_3CH_2F[d]	F	9.75	−0.75	−0.41
$CH_3CH_2PH_2$[d]	PH_2	16.41	+0.59	+0.14
	H(P)[e]	1.58	−0.58	−0.08

[a] Wave functions generated with the 6-31(+)G** or 6-31G** basis set. [b] Integrated population from volumes defined with the Bader procedure. [c] Sum of populations on phosphorus and two hydrogens. [d] Structures optimized at the 6-31G* level in staggered conformations. [e] Average of two hydrogens.

(37) Complex 5 contains a negative frequency of −35 cm^{-1}. The potential energy surface is very flat for this complex and repeated attempts at complete optimizations led to slow convergence problems. To avoid these difficulties, a C_s symmetry structure was optimized. The difference in energy between this structure and the fully optimized structure should be negligible. In addition, structures with the hydrogens of PH_2^- interacting with ethyl chloride were investigated. These structures were slightly less stable than 5.

(38) Hammond, G. S. *J. Am. Chem. Soc.* **1955**, *77*, 334.

(39) Determined at the MP4SDQ/6-31(+)G**//HF/6-31G* level of theory. Experimental value is −29.5 kcal/mol, see: Pedley, J. B.; Rylance, J. *Sussex-N.P.L. Computer Analyzed Thermochemical Data: Organic and Organometallic Compounds*; University of Sussex: Sussex, England, 1977. Also see ref 22.

(40) Bader, R. F. W.; Duke, A. J.; Messer, R. R. *J. Am. Chem. Soc.* **1973**, *95*, 7715.

Table III. Critical Point Densities[a]

structure	bond	ρ, e/au^3	structure	bond	ρ, e/au^3
2	C–F	0.037	**7**	H_2P–H_β	0.069
	C–CL	0.061		C–H_β	0.148
3	F–H_β	0.143		C–C	0.320
	C–H_β	0.149		C–Cl	0.039
	C–C	0.301	**8**	H_2P–H_β	0.066
	C–Cl	0.064		C–H_β	0.153
4	F–H_β	0.195		C–C	0.311
	C–H_β	0.103		C–Cl	0.050
	C–C	0.281	CH_3CH_2F[b]	C–F	0.231
	C–Cl	0.097	$CH_3CH_2PH_2$[b]	H_2P–C	0.155
6	C–P	0.025	CH_3CH_2Cl[b]	C–H_β	0.286
	C–Cl	0.054		C–C	0.262
				C–Cl	0.178

[a] Critical points derived with the Bader approach with 6-31(+)G** and 6-31G** basis sets. [b] Optimized at the 6-31G* level in staggered conformation.

cause bond distances are long and interatom electron densities are small in transition states, basis set superposition errors are limited and Mulliken populations parallel integrated populations.

It has been shown that bond orders can be analyzed by considering the electron density (ρ) at the critical point of the bond.[41] The critical point represents the minimum in electron density along the bond axis. Intuitively, one would expect the density at this point to reflect the amount of shared electron density and therefore the strength of the covalent interaction. Of course the absolute values of ρ depend on a number of factors, including the sizes of the bonded atoms, but relative values give a reasonable measure of bonding changes during a chemical reaction. For example, the weakness of the C–Cl bond in **2** can be assessed with this method. In the S_N2 transition state (Table III), the critical point density (ρ) is only 0.061 as compared to 0.178 in the parent CH_3CH_2Cl, indicating that much of the shared density has already shifted to the chlorine.[42] Although the C–Cl bond has only slightly stretched, there already has been a significant electronic reorganization. The forming C–F bond in **2** has a ρ value of only 0.037 and consequently there is little shared density or covalent bonding. For comparison, the ρ value for the C–F bond in CH_3CH_2F is 0.231.

A similar S_N2 transition-state geometry is found for PH_2^- + CH_3CH_2Cl (**6**). Here, because the P–H bonds interact with C–H bonds on the α-carbon, the transition state lacks C_s symmetry. The C–P bond is exceptionally long, 2.99 Å, and again an early transition state is observed.[43] The leaving chlorine has nearly the same electron population (17.73 e$^-$) as in **2** and the PH_2^- fragment has transferred some of its population (18 e$^-$ in PH_2^- compared to 17.75 in **6**). The result is a net charge of +0.48 on the CH_3CH_2 fragment. Once again the charges reflect Bader's generalization;[40] in S_N2 reactions, the entering and leaving nucleophiles carry significant negative charge while the carbon is somewhat positive. The system is stabilized by the electrostatically favorable ion triplet (− + −) character.

The energies of the S_N2 transition states were calculated at various levels and are listed in Table IV. At the MP4SDQ/6-31(+)G**//HF/6-31(+)G* level, the transition state for the S_N2 reaction of F^- and CH_3CH_2Cl (**2**) is 6.7 kcal/mol below the energy of the separated reactants, or in other words about 8 kcal/mol above complex **1**. This yields the typical Brauman double-welled potential picture (Figure 3) of a gas-phase S_N2 reaction where the complexation energy is used to overcome the activation barrier and a negative activation energy is possible.[12] The effect of correlation in these calculations is significant and leads to larger barriers for the S_N2 reaction. The present values may be compared with those of Minato and Yamabe,[16] who at lower levels of theory

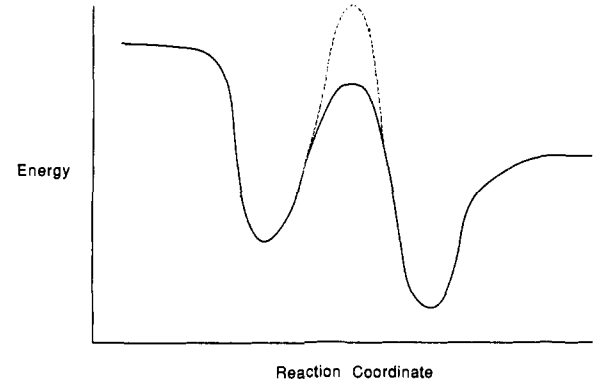

Figure 3. Sample potential energy diagrams for gas-phase reactions: (—) negative activation barrier; (---) positive activation barrier.

found the transition state to lie between 8.9 and 17.2 kcal/mol below the energy of the separated reactants. Using a large basis set and MP2 corrections, Shi and Boyd[18] observed a more negative S_N2 activation barrier (−7.8 kcal/mol) for the reaction of F^- with CH_3Cl, indicating that the steric bulk of the extra methyl group in **2** has a modest effect on the energy of the transition state (barrier = −4.8 kcal/mol at the MP2 level). Because the energy of **2** is significantly lower than that of the reactants, the reaction should be viable in the gas phase. In fact, F^- is known to undergo a very rapid and efficient (efficiency = 0.56) substitution reaction with methyl chloride in the gas phase.[7] The efficiency of a reaction is the observed rate divided by the theoretical collision rate, or in other words the fraction of ion–molecule collisions that actually lead to products. An efficient reaction also is seen in the gas phase for F^- + ethyl chloride, but the ratio of substitution to elimination is not known for this system.

The energies of the PH_2^- + CH_3CH_2Cl S_N2 transition state also are listed in Table IV. At the MP4SDQ/6-31(+)G**//HF/6-31(+)G* level, **6** is 5.8 kcal/mol above the energy of the separated reactants. As a result, the S_N2 reaction of PH_2^- has a positive activation energy. Moreover, the PH_2^- transition-state barrier is much larger than the one that is observed with F^-. DePuy and co-workers[44] have found that the gas-phase reaction of PH_2^- and CH_3Cl is relatively inefficient (efficiency = 0.056), indicating that this S_N2 reaction has a significant barrier.

E2 Transition States (Anti). From complex **1**, an E2 anti elimination reaction of F^- and CH_3CH_2Cl also is possible. The transition state, **3**, for the elimination reaction is characterized by a nearly linear C–H_β–F configuration and a long C–H_β distance of 1.35 Å. The F–H_β distance (1.21 Å) also is relatively long, yielding a transition state where the transferring hydrogen is roughly midway between the carbon and fluorine and the proton transfer is approximately half completed. The C–Cl bond has stretched to 2.22 Å, approximately the same length that was observed in the S_N2 transition state, **2**. In fact the geometry about the α-carbon is very similar to that in the S_N2 and E2 transition states. The C–C bond (1.42 Å) in **3** is much shorter than that in ethyl chloride (1.52 Å), indicating partial double bond formation. In addition, the hybridization of the carbons has changed to yield a more planar CH_2CH_2 fragment. This transition state, therefore, is fairly consistent with the prototypic E2-type mechanism where proton transfer, double bond formation, and expulsion of the leaving group occur simultaneously. In contrast, Dewar[19] found that the reaction of methoxide with ethyl chloride has a more $E1_{cb}$-like mechanism; there is virtually no C–Cl bond elongation in the transition state (C–Cl = 1.84 Å). This may be the result of using a more basic nucleophile (methoxide proton affinity = 380.6 kcal/mol)[22] or it also may be an artifact of the semiempirical technique. Although complex **1** is perfectly poised for a Winstein–Parker E2C-type pathway, the linearity of the proton transfer in **3** eliminates this possibility.[3]

(41) For example, see: (a) Knop, O.; Boyd, R. J.; Choi, S. C. *J. Am. Chem. Soc.* **1988**, *110*, 7299. (b) Bader, R. F. W.; Slee, T. S.; Cremer, D.; Kraka, E. *J. Am. Chem. Soc.* **1983**, *105*, 5061.

(42) In the text, critical point densities are reported in units of e$^-$/au^3.

(43) Exothermicity = 41.6 kcal/mol at the MP4SDQ/6-31(+)G**//HF/6-31G* level.

(44) Anderson, D. R.; Bierbaum, V. M.; DePuy, C. H. *J. Am. Chem. Soc.* **1983**, *105*, 4244.

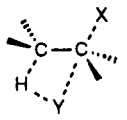

E2C

A similar transition-state structure, **7**, is seen in the anti-elimination reaction of PH_2^- and CH_3CH_2Cl. The P–H_β distance is long (1.92 Å) and the proton transfer involves a nearly linear geometry. Relative to **3**, there is greater double bond character as evidenced by a shorter C–C bond length (1.39 Å). The longer C–Cl distance (2.46 Å) indicates that relative to the fluorine system, **3**, proton transfer is lagging behind Cl^- expulsion. This can be interpreted as evidence of a more $E1_{cb}$-like mechanism when F^- is the nucleophile.

The charge distributions for the transition states are listed in Table II. In **3**, the fluorine maintains nearly a full negative charge (pop. = 9.88 e^-), but the transferring proton has lost much of its population going from 1.06 e^- in CH_3CH_2Cl to only 0.42 e^- in **3**. The charge release from the transferring hydrogen is partly compensated by a population increase on the leaving Cl (pop. = 17.71 e^-), but the net result is a buildup of charge on the CH_2CH_2 fragment in the transition state.

The electron distribution in the transition state of the PH_2^- induced elimination produces a different pattern. In particular, the PH_2^- population is significantly reduced in the transition state (17.60 e^- in **7**, 18.0 e^- in PH_2^-) and a more modest population reduction is observed on the transferring hydrogen (pop. = 0.76 e^-). This result can be rationalized if one considers the total populations of the H_2P–H_β and F–H_β fragments in the E2 transition states. Although the distributions within the fragments are different, the net charges on them are very similar, −0.36 on H_2P–H_β and −0.30 on F–H_β. As a result, the CH_2CH_2Cl fragment has virtually the same population in both transition states. The larger positive charge on the transferring hydrogen in **3** is simply a reflection of the difference in polarization of F–H and P–H bonds.

$$\overset{\delta^+\ \delta^-}{R_2P{-}H} \qquad \overset{\delta^-\ \delta^+}{F{-}H}$$

Consistent with the longer C–Cl bond observed in **7**, the leaving Cl has a larger electron population (pop. = 17.81 e^-) and a lower ρ value than was observed in **3**. Finally, as noted with the S_N2 transition states Mulliken populations tend to parallel Bader integrations; however, major differences are observed in the P–H and C–H bonds where Mulliken populations overestimate the density on phosphorus and carbon, respectively.

The electron population of the transferring hydrogen in **7** presents an interesting dilemma. In CH_3CH_2Cl, the electrons in the C–H bonds are shared equally and each hydrogen has a population of about 1.0 e^-. In contrast, P–H bonds are significantly polarized with excess density residing on the hydrogens (pop. = 1.61 in PH_3). Therefore, the transferring hydrogen should eventually experience a population increase as the conversion of C–H to P–H bond proceeds. However, because the elimination process formally involves a proton transfer, at the transition state the transferring hydrogen experiences a population decrease and must accept a slight positive charge. In other words, the charge on the hydrogen does not smoothly change from reactants to products and acts as a nonlinear reaction coordinate.

The energies of the anti-elimination transition states are given in Table IV. In these reactions, only small correlation effects are observed. At the MP4SDQ/6-31(+)G**//HF/6-31(+)G* level, the transition state for the fluoride-induced anti elimination of CH_3CH_2Cl lies 5.7 kcal/mol below the energy of the separated reactants, virtually the same energy as the S_N2 transition state, **2**. Therefore, both the E2 and S_N2 processes have similar potential energy diagrams and are viable when F^- is the nucleophile. The E2 barrier may be compared to those from Minato and Yamabe.[16] Depending on the level of theory they used, values ranging from 9 kcal/mol below to 0.5 kcal/mol above the energy of the separated reactants were reported. The negative activation barrier for the elimination reaction is consistent with the experimental observation that F^- reacts readily with primary as well as secondary and tertiary alkyl chlorides in the gas phase.[7]

In contrast, an exceptionally large barrier is observed for the PH_2^- induced anti elimination. At the highest level of theory, **7** lies 17.4 kcal/mol above the energy of the separated reactants. This large barrier guarantees a very slow rate for the gas-phase reaction. Whereas the S_N2 and E2 reactions of F^- had similar barriers, the E2 barrier for PH_2^- is 12 kcal/mol above the S_N2 barrier. As a result, PH_2^- is a poor nucleophile for S_N2 reactions and essentially an ineffectual base for E2 eliminations. Although the overall exothermicities of F^- and PH_2^- induced eliminations are similar,[45] the transition-state barriers differ by 23 kcal/mol. In other words, PH_2^- and F^- have similar thermodynamic basicities, but much different kinetic basicities. There are no examples of gas-phase PH_2^- induced eliminations of alkyl halides, but as stated earlier, other second-row nucleophiles such as HS^- and H_2NS^- are poor bases for E2 reactions.

E2 Transition States (Syn). The transition states for the F^-, **4**, and PH_2^-, **8**, induced syn eliminations of CH_3CH_2Cl are given in Figure 2. Ion–dipole complexes leading to these transition states were not located. The geometry differences between transition states **4** and **3** are clearly consistent with the syn elimination process involving a transition state with more $E1_{cb}$ character. First, proton transfer has progressed to a much greater extent in **4** as evidenced by a longer C–H_β distance (1.47 Å) and a shorter F–H_β distance (1.10 Å). In addition, the C–Cl bond length is shorter in **4**, indicating that Cl^- expulsion has occurred to a lesser extent. Finally, the long C–C bond (1.46 Å) in **4** is consistent with reduced double bond formation at the transition state. An enlarged H_β–C–C angle (121°) is evidence of an unfavorable interaction between the developing carbon lone pair and the C–Cl bond.

The enhanced $E1_{cb}$ character of transition state **4** can be confirmed by examining the charge distribution. In **4**, the lagging Cl expulsion is characterized by a larger ρ value (C–Cl) and a smaller chlorine population (17.58 e^-) than is present in **3**. In addition, the β-carbon in **4** has a slight negative charge (pop. = 6.16 e^-) which is consistent with the partial carbanion character expected for an $E1_{cb}$ transition state. For comparison, the populations of the β-carbons in **3** and CH_3CH_2Cl are 5.99 and 5.76 e^-, respectively.

When PH_2^- is the nucleophile, the differences between anti (**7**) and syn (**8**) elimination geometries are less dramatic. In **8**, the C–H_β (1.31 Å) and C–C (1.41 Å) bonds are longer and the C–Cl (2.36 Å) bond is shorter; however, all the differences are quite small. As in the S_N2 transition state, long-range interactions of the P–H bonds lead to a structure without C_s symmetry.

The energies of the syn transition states are given in Table IV. At the MP4SDQ/6-31(+)G**//HF/6-31(+)G* level, the transition state for the F^- induced syn elimination of CH_3CH_2Cl lies 7.0 kcal/mol above the energy of the separated reactants or 12.7 kcal/mol above the energy of the anti transition state. Minato and Yamabe[16] found a similar energy difference between syn and anti pathways. In addition, de Koning and Nibbering have studied the gas-phase reactions of strong bases with ethers and have found indirect evidence that anti eliminations are favored.[10e] Moreover, there is ample evidence that the syn geometry is less efficient in promoting E2 eliminations in solution.[5] Given the difference in energy, the syn pathway is probably insignificant in the gas-phase reaction of F^- with ethyl chloride. For PH_2^-, the syn transition state lies 25.8 kcal/mol above the energy of the separated reactants or 8.4 kcal/mol above the anti-elimination transition state. Once again anti is significantly favored. In this case, however, neither elimination pathway is energetically viable in the gas phase.

S_N2 vs E2. The competition between S_N2 and E2 pathways has been considered in a variety of gas-phase experiments, but rarely has it been possible to develop definitive structure–reactivity relationships.[7-10] The difficulty is that most of these experiments are based on mass spectrometry so only ionic products are detected

(45) The exothermicities of the E2 reactions are approximately −19.5 kcal/mol for both F^- and PH_2^-, see refs 22 and 39.

Table IV. Energies of Minima and Transition States[a]

	6-31(+)G*	6-31(+)G**			
structure	HF	HF	MP2	MP3	MP4(SDQ)
		Fluoride Reactions			
1	−637.578 78	−637.584 17	−638.214 06	−638.240 54	−638.254 36
	(−15.4)	(−15.7)	(−14.9)	(−15.3)	(−15.1)
2	−637.567 83	−637.576 26	−638.197 69	−638.224 25	−638.240 51
	(−10.6)	(−10.8)	(−4.8)	(−5.4)	(−6.7)
3	−637.550 79	−637.562 37	−638.195 51	−638.219 82	−638.233 15
	(−3.5)	(−5.9)	(−7.1)	(−6.2)	(−5.7)
4	−637.528 17	−637.540 80	−638.175 20	−638.201 18	−638.212 76
	(+10.0)	(+7.5)	(+5.5)	(+5.4)	(+7.0)
		Phosphide Reactions			
5	−879.997 63	−880.010 24	−880.559 88	−880.614 22	−880.621 52
	(−7.3)	(−7.3)	(−7.9)	(−7.8)	(−7.7)
6	−879.975 51	−879.988 30	−880.536 94	−880.589 85	−880.599 79
	(+6.5)	(+6.3)	(+6.4)	(+7.4)	(+5.8)
7	−879.943 96	−879.958 36	−880.518 03	−880.567 06	−880.575 97
	(+22.9)	(+21.7)	(+14.9)	(+18.3)	(+17.4)
8	−879.925 22	−879.939 11	−880.505 56	−880.554 05	−880.563 07
	(+34.9)	(+34.1)	(+23.0)	(+26.8)	(+25.8)
CH_3CH_2Cl	−538.132 48	−538.140 26	−538.566 16	−538.602 21	−538.606 56

[a] Absolute energies given in hartrees. Energies relative to the separated reactants given in parentheses (kcal/mol). Structures from 6-31(+)G* or 6-31G* optimizations. See Table I for energies of nucleophiles.

and S_N2 and E2 pathways cannot be distinguished directly (both mechanisms give the same ionic product, see Figure 1). Two studies have investigated the neutral products of gas-phase nucleophilic reactions. Jones and Ellison[8] collected the neutral products from the reaction of methoxide with *n*-propyl bromide and found only the elimination product, propene. Lieder and Brauman[9] studied the neutral products from the reaction of fluoride with ethyl chloride. Here, ethyl fluoride was observed, but it was not possible to determine if elimination products also were present. In systems where the structure of the ionic product is characteristic of the mechanism, elimination products only or mixtures of elimination and substitution products have been observed.[10] The recent kinetic and isotopic studies of DePuy et al.[7] (see above) show the clearest relationship between the structure of the nucleophile and the preference for S_N2 or E2 pathways.

The ab initio studies yield the structures and energies of the transition states of the E2 and S_N2 reactions so it is possible to make some qualitative predictions about the competition between the two mechanisms. First, a brief discussion of the energetics of gas-phase ion–molecule reactions is appropriate. Reactions with negative activation barriers (Figure 3) are expected to be very fast in the gas phase, but because entropic barriers may be present, negative activation barriers do not always lead to reactions with unit efficiency.[12] Reactions with positive activation barriers are generally slow because they face both enthalpic and entropic barriers. For a variety of practical reasons, gas-phase rates may be measured only for relatively fast reactions (efficiency > 0.0001).[7,13] Therefore only reactions with negative or slightly positive activation barriers (<4–6 kcal/mol) can be characterized.

For the reaction of F^- with CH_3CH_2Cl, three reaction paths were investigated theoretically, S_N2, E2(anti), and E2(syn). The S_N2 and E2(anti) reaction transition states have energies that are approximately 6 kcal/mol below that of the separated reactants and, therefore, neither path has an enthalpic barrier. Because the E2(syn) reaction involves a significant barrier (7 kcal/mol), it should not be competitive with the more facile S_N2 and E2(anti) reactions. Since the energies of the S_N2 and E2(anti) transition states are essentially the same, the preference for an E2 or S_N2 pathway is based on the entropic constraints of the transition states. Brauman[12] has pointed out that the S_N2 transition state is highly ordered and entropically unfavorable. Consequently, even S_N2 reactions with significant negative activation barriers may face entropic barriers that reduce the rate below the collision-controlled limit. In contrast, the E2 transition state is relatively free and suffers fewer entropy constraints. The flexibility of the E2 transition state is verified by the presence of low frequency bending modes (88 and 89 cm^{-1}) associated with the proton transfer (the lowest frequencies in the S_N2 transition state are 161 and 187 cm^{-1}). Assuming the E2 reaction is entropically favored, the theoretical results predict that both the S_N2 and E2(anti) paths are viable, but the E2(anti) path will most likely dominate. A mixture of substitution and elimination is consistent with Brauman's experimental observation of ethyl fluoride in the reaction of fluoride with ethyl chloride.[9] In addition, this interpretation is consistent with gas-phase kinetic studies of the reactions of F^- with other alkyl chlorides. Fluoride reacts readily with CH_3Cl (efficiency = 0.56), but even more readily with CH_3CH_2Cl, $(CH_3)_2CHCl$, and $(CH_3)_3CCl$ (efficiencies from 0.79 to 0.93).[7] Clearly the S_N2 reaction is viable, but the rate increases with ethyl, isopropyl, and *tert*-butyl chloride can only be explained by the presence of an E2 pathway. Finally, the reactivity pattern for F^- is similar to that observed for the fluorinated alkoxides whose gas-phase E2 reactions were confirmed with kinetic deuterium isotope effects (see above).

In the reaction of PH_2^- with CH_3CH_2Cl, the options are more limited. All of the pathways have positive activation barriers with the smallest being +5.5 kcal/mol for the S_N2 reaction. The two E2 reactions have very large activation barriers (over 17.4 kcal/mol) which effectively eliminate the possibility of an observable gas-phase reaction. Therefore, PH_2^- is capable of a slow S_N2 reaction with CH_3CH_2Cl, but no E2 eliminations are expected under typical gas-phase conditions. The absence of E2 reactivity with PH_2^- is not a thermodynamic artifact because E2 reactions of PH_2^- and F^- are equally exothermic. Both the nucleophiles, F^- and PH_2^-, have the same thermodynamic basicities in the gas phase, but apparently PH_2^- is a much weaker kinetic base. Assuming that further substitution will retard the S_N2 reaction, one would expect PH_2^- to react very sluggishly with secondary and tertiary alkyl chlorides (the E2 is so unfavorable with CH_3CH_2Cl that increased substitution should not make the elimination reaction viable). This reactivity pattern is similar to what DePuy et al. observed for the reactions of sulfur nucleophiles with alkyl chlorides.[7] H_2NS^- and HS^- react readily with methyl chloride, but reaction rates drop dramatically along the series ethyl, isopropyl, and *tert*-butyl chloride.

The large difference in the relative kinetic and thermodynamic basicities of these nucleophiles offers insight into Winstein and Parker's E2C transition state.[3] For soft nucleophiles, they found no correlation between E2 rates and nucleophile basicity; however, the E2 rates for these nucleophiles do correlate with S_N2 rates. This led them to postulate that the nucleophile was interacting with the α-carbon. The present theoretical results show that no correlation between thermodynamic basicity and E2 rate should be expected. The *kinetic basicity* is the deciding factor, and it is not surprising that kinetic basicity correlates with S_N2 reactivity. Although F^- and PH_2^- have the same thermodynamic basicities,

their kinetic reactivities are very different. With PH_2^-, the activation barriers for S_N2 and E2 reactions are both larger than those found with F^-. This results in a correlation (albeit a two point correlation) between S_N2 and E2 rates even though the E2 transition states exhibit no interaction between the nucleophile and the α-carbon.[46] The linear proton transfer geometry is preferred in the transition state because it minimizes electrostatically unfavorable interactions between the nucleophile and the developing carbanion.

First-Row vs Second-Row Nucleophiles. Although only a representative first- and second-row nucleophile was considered, some useful generalizations can be developed. The validity of such generalizations is strengthened by the fact that the theoretical results with F^- and PH_2^- parallel DePuy's gas-phase studies with fluorinated alkoxides and sulfur-based nucleophiles.[7]

From the theoretical studies, PH_2^- is clearly a much weaker nucleophile than F^- in both S_N2 and E2 reactions. That is, there is a larger kinetic barrier for PH_2^- to form new bonds to carbon and hydrogen. One might argue that the enhanced reactivity of fluoride and other first-row nucleophiles is simply a manifestation of Pearson's hard-soft acid principle[47] where the proton in the E2 reaction and the carbon in the S_N2 reaction act as hard acids. However, by examining the shifts in electron density distributions as the reactions occur, a more graphical explanation for the difference in reactivity of F^- and PH_2^- can be developed.

In the transition state of the S_N2 reaction of F^- and CH_3CH_2Cl, the fluoride is in the process of donating one of its lone pairs to form a new bond to carbon. The bond is highly polarized so even in the product, CH_3CH_2F, the fluoride (pop. = 9.75 e^-) retains much of its original population. In contrast, when PH_2^- undergoes an S_N2 reaction the phosphorus must shift most of its lone pair density onto the carbon because carbon is effectively more electronegative than phosphorus.

$$R_3C^{\delta-}\!\!-\!\!P^{\delta+}H_2$$

The electron population on the PH_2 fragment shifts from 18.00 (net charge = −1.00) to 16.41 (net charge = +0.59) in going from reactants (PH_2^-) to products ($CH_3CH_2PH_2$). The greater electronic reorganization required for this S_N2 process is the cause of the larger activation barrier. The problem in bond polarity also can be illustrated by taking advantage of microscopic reversibility. Obviously the same kinetic barriers encountered in the reaction of PH_2^- with CH_3CH_2Cl will be found in the back-reaction of Cl^- with $CH_3CH_2PH_2$. Before Cl^- can expel PH_2^- from $CH_3CH_2PH_2$, the C–P bond polarity must reverse to shift the density onto phosphorus. Intuitively, this shift in polarity should involve a significant barrier. In the analogous back-reaction of Cl^- with CH_3CH_2F, the C–F bond already has the proper polarity and only a small shift in density is required for the fluorine to leave smoothly as F^-.

This argument can be extended to E2 reactions. As noted earlier, the P–H bond is polarized with most of the density near hydrogen. When PH_2^- initiates the proton transfer of the E2 mechanism, the transferring hydrogen must leave the carbon as a proton, but eventually take on hydride character as the P–H bond is formed. The result is an unusual shift in population from 1.06 electrons in CH_3CH_2Cl to 0.76 electron in transition state **7**, and finally to 1.61 electrons in the product, PH_3. In essence, the phosphorus is trying to donate its lone pair to the hydrogen at the same time as the hydrogen is releasing its C–H bond density to carbon—the net result is extensive electron–electron repulsions in the transition state and a large activation barrier. The problem in electron flow is clear once one realizes that as the proton transfer progresses, a carbon lone pair is formed in close proximity to a hydrogen with developing hydride character. In a sense, we have an anti hydrogen bond (the polarity is reversed). For the F^- induced elimination, the forming F–H bond is polarized with most of the density on fluorine so as the reaction proceeds the hydrogen smoothly releases the C–H bond density onto carbon and adopts the protic character found in HF. As the carbon lone pair develops it is stabilized by a favorable hydrogen-bonding interaction with the HF. The result is a relatively small activation barrier.

Since all of these arguments have been couched in terms of bond polarity, they may be generalized. Second-row elements are inherently less electronegative than first-row elements and therefore, to some extent, will be at a disadvantage in terms of bond polarity. Second-row elements such as Si, P, and S form bonds to carbon and hydrogen with most of the shared density polarized away from the second-row element. This represents a reversal in polarity because generally the nucleophilic site in a base is more electronegative than the atom it attacks (C or H). As a consequence of this reversed polarity, second-row nucleophiles generally will require greater electronic reorganizations in S_N2 and E2 reactions and as a result encounter larger activation barriers. Finally, all these arguments involve intrinsic nucleophilicity and are only valid in the gas phase or under conditions where differential solvation of first- and second-row nucleophiles is not important.

Conclusion

These theoretical studies provide further evidence that first- and second-row nucleophiles of similar basicity have marked differences in their ability to undergo S_N2 and E2 reactions. The S_N2 and E2(anti) reactions of F^- with CH_3CH_2Cl have negative activation barriers and both pathways are viable under typical gas-phase reaction conditions. In contrast, the S_N2 reaction of PH_2^- with CH_3CH_2Cl has a small positive activation barrier and the E2 processes have very large activation barriers. As a result, PH_2^- is capable of only a slow S_N2 reaction. For both systems, the E2(anti) is significantly favored over the E2(syn), indicating that an antiperiplanar transition state is preferred in the gas phase.[48] The inability of PH_2^- to induce an elimination reaction can be understood by examining the bond polarities. Because the P–H bond is naturally polarized with greater density around hydrogen, the hydrogens in phosphine have some inherent hydride character. In the E2 process the transferring hydrogen must leave as a proton, but eventually develop hydride character as the P–H bond forms. This unusual electron flow leads to electron–electron repulsions which destabilize the transition state. Since all second-row nucleophilic centers are less electronegative than first-row nucleophilic centers of similar gas-phase basicity, they will be at a disadvantage in E2 reactions. This reversal in bond polarity (hydrogen or carbon being more electronegative than the nucleophilic center) also affects the S_N2 reaction, but to a lesser extent. Further research on substituent and leaving group effects in the E2 reaction has been completed and will be published in subsequent papers.[48]

Acknowledgment. The Multi-Flow Trace/14 computer used for these calculations was purchased on a grant from the Chemical Instrumentation Program of the National Science Foundation (CHE-8822716). I would like to thank Professor R. F. W. Bader and his research group for providing a copy of their Proaim package. I also would like to thank Professor C. H. DePuy and Dr. V. M. Bierbaum for their many helpful discussions concerning the gas-phase kinetics and isotope effects of the ion–molecule reactions.

Supplementary Material Available: Listing of Z matrix elements, energies, and frequencies (9 pages). Ordering information is given on any current masthead page.

(46) Correlations between S_N2 rates and kinetic rather than thermodynamic acidities are also evident with resonance delocalized anions, see: (a) Dodd, J. A.; Brauman, J. I. *J. Am. Chem. Soc.* **1984**, *106*, 5357. (b) Han, C.-C.; Brauman, J. I. *J. Am. Chem. Soc.* **1989**, *111*, 6491.

(47) (a) Pearson, R. G. *Surv. Prog. Chem.* **1969**, *5*, 1. (b) Pearson, R. G.; Songstad, J. *J. Am. Chem. Soc.* **1967**, *89*, 1827. (c) Pearson, R. G. *J. Am. Chem. Soc.* **1963**, *85*, 3533.

(48) In these systems, prototypic E2 transition-state geometries were observed. Other work indicates that the preference is diminished in more $E1_{cb}$-like systems; Gronert, S. Manuscript in preparation.